Cell

Contingency and Statistical Laws in Replicate Microbial Closed Ecosystems

Doeke R. Hekstra[1,3,*] and Stanislas Leibler[1,2]
[1]Center for Studies in Physics and Biology and Laboratory of Living Matter, The Rockefeller University, 1230 York Avenue, New York, NY 10065, USA
[2]The Simons Center for Systems Biology and The School of Natural Sciences, Institute for Advanced Study, Einstein Drive, Princeton, NJ 08540, USA
[3]Present address: Green Center for Systems Biology, University of Texas Southwestern Medical Center, Dallas, TX 75390, USA
*Correspondence: doeke.hekstra@utsouthwestern.edu
DOI 10.1016/j.cell.2012.03.040

SUMMARY

Contingency, the persistent influence of past random events, pervades biology. To what extent, then, is each course of ecological or evolutionary dynamics unique, and to what extent are these dynamics subject to a common statistical structure? Addressing this question requires replicate measurements to search for emergent statistical laws. We establish a readily replicated microbial closed ecosystem (CES), sustaining its three species for years. We precisely measure the local population density of each species in many CES replicates, started from the same initial conditions and kept under constant light and temperature. The covariation among replicates of the three species densities acquires a stable structure, which could be decomposed into discrete eigenvectors, or "ecomodes." The largest ecomode dominates population density fluctuations around the replicate-average dynamics. These fluctuations follow simple power laws consistent with a geometric random walk. Thus, variability in ecological dynamics can be studied with CES replicates and described by simple statistical laws.

INTRODUCTION

Biology has an important historical component. Individual events can often influence the course of biological phenomena in a crucial, lasting way. For example, it has been argued that the impact of a giant meteorite or a series of volcanic eruptions could have modified our environment and led to massive extinctions, suggesting that the Earth's biome could have been influenced by random geophysical or astrophysical events. Such historical contingency does not have to be due only to such extrinsic influences. Stochastic intrinsic events, from molecular noise leading to genetic mutations to random interactions between different organisms in an ecosystem, can change the detailed history of biological evolution (Blount et al., 2008).

This historical nature of evolution was summarized in a now famous question: would intelligent humans evolve again if the tape of evolution could have been rewound and played again (Gould, 1989)? Because such an experiment is obviously out of reach, this question quickly became the subject of lively arguments, with proponents of pure contingency opposing scientists who point to many cases of evolutionary *convergence*, in which different paths, influenced by random events, still lead to similar outcomes (Morris, 2010). This type of issue seems to emerge in many sciences, such as ecology, geology, or economics, that deal mostly with unique temporal progressions that are impossible to reproduce or observe all over again in detail. It is possible that, despite all efforts to make these sciences mathematical, our description of observed long-term ecological, geological, or economic phenomena will remain largely narrative, evoking many detailed events that influenced each particular history (Mrozek, 1968).

There remains, however, the possibility that, even in these complex systems involving many interacting components, simple quantitative laws can emerge at some spatial and temporal scales (Bak and Paczuski, 1995). The Gutenberg-Richter law in geology, which shows that the distribution of earthquakes follows a simple power-law or scale-free behavior, is a powerful example of such emergent laws. Accordingly, although the occurrence of an earthquake of a given magnitude at a given time and place depends on an enormous number of unknown and largely historical details, the statistical law describing its occurrence is simple and universal (Carlson and Langer, 1989). Even if detailed prediction of earthquakes remains beyond reach (especially for longer time intervals), one can still use this law to prepare for likely future events. Importantly, the Gutenberg-Richter law has also been reproduced in laboratory experiments studying "stick-slip phenomena," (Bretz et al., 2006) thus contributing to better understanding of the mechanical origins of earthquakes. Similarly, a series of experiments on charged density waves, Barkhausen noise in magnets, and other systems leads to the emergence of a more unifying view of so-called "crackling noise," of which earthquakes are only one of many examples (Sethna et al., 2001).

Box 1. The Advantage of Replicate Time Series

Imagine a set of time series for two interacting, hypothetical species S_1 and S_2 (panel A; for this example, we use n = 19 artificial time series with known dynamics; for details, see Supplemental Information). Their true density dynamics are stochastic, and they have a slowly changing average. A central difficulty in ecology is that most time series are unique; they are acquired under conditions that are not readily replicated. Fluctuations, however, are only well defined with respect to a reference. For example, the so-called interaction matrix B, which describes the correlations in the density fluctuations of the two species, can be estimated by regression of $\log(n/n^{ref})$ at time $t + \Delta t$ onto $\log(n/n^{ref})$ at time t, with $n = (n_{S_1}, n_{S_2})$ and $n^{ref}(t)$ the reference dynamics (Ives, 1995). For unique time series, one is thus forced to make a *guess* about $n^{ref}(t)$. Common choices include $n^{ref}(t)$ = constant or an exponential trend $n^{ref}(t) = n^{ref}(0) \cdot e^{-t/\tau}$ fitted to each time series. We illustrate this usual approach by treating each pair of time series (n_{S_1}, n_{S_2}) as unique while estimating B (panel B) for the two-species artificial data. Fluctuations of S_1 around its fitted exponential trend are plotted against those of S_2 (shown in detail for one pair of time series as the black "trajectory"; for other pairs of time series, we only show time points as gray dots). It is clear that the estimated eigenvectors of B and the corresponding eigenvalues λ_B deviate substantially from the known true values (the directions of *estimated* eigenvectors are shown as brown lines, and $1-\lambda_B$, which measure the degree of reversion to the mean, are depicted as brown arrows. The gray lines and arrows correspond to *true* eigenvectors and eigenvalues).

If, instead, the same data are considered to come from *replicate* ecosystems, one can properly estimate the reference dynamics, $\log n^{ref}(t)$, as the replicate-average dynamics, $\langle \log n(t) \rangle$ (thick red and blue lines, C; shown here with ±1 SD colored areas), yielding much better estimates of the eigenvectors and eigenvalues of B (green lines and arrows in D). Similar considerations hold true for other dynamical properties, such as the Hurst exponent (Figure 5A).

Moreover, creating replicate ecosystems offers an alternative perspective on the biological constraints governing ecological dynamics. Variation between replicates at a single point in time (E) permits estimation of a covariance or correlation matrix (F). For our experimental data, we show that the eigenvectors of the correlation matrix (which we call ecomodes; Figure 4) stabilize over time and approximate the eigenvectors of the interaction matrix B (compare, for illustration, the structure of E and F). The corresponding eigenvalues of B closely resemble autoregressive coefficients, b, describing fluctuations along the ecomodes (Figure 4C).

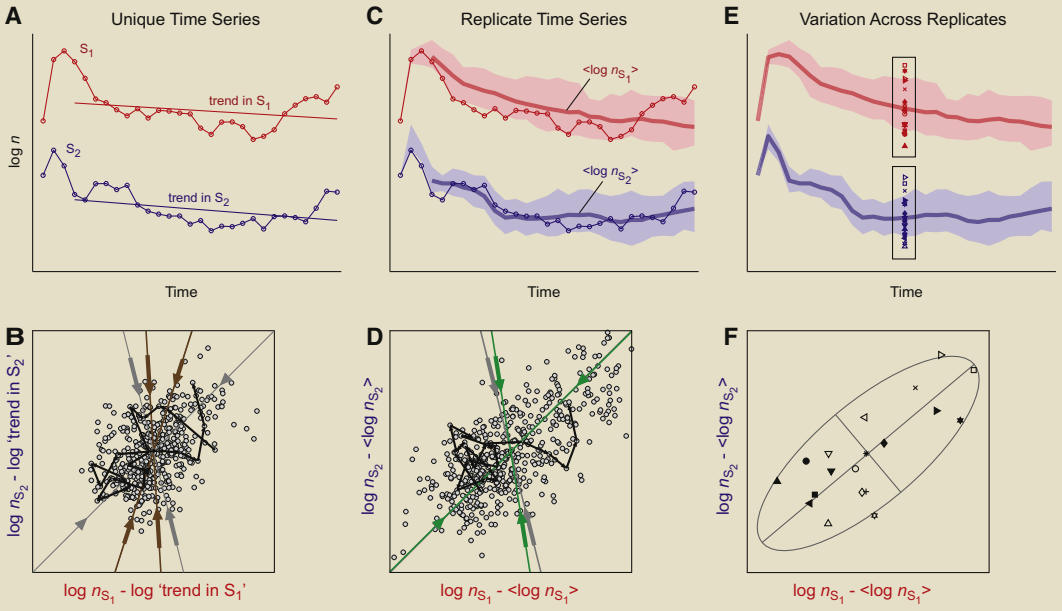

The study of the statistical properties of population dynamics is a good starting point for the search for such emergent laws in ecology. Time series for populations of interacting species in an ecosystem often exhibit large temporal variations. Separating the average behavior from random fluctuations is simply impossible for any single time series (Box 1). Quantitative laboratory experiments are thus required because they can be performed in replicate under the same controlled conditions. This type of experiment, measuring microbial population dynamics in many replicates of the same ecosystem under well-controlled external conditions, is the focus of the present work.

Ecosystems that were closed to material transport but open to energy flow (in particular, illumination allowing for photosynthesis) were first developed as part of space programs with the goal of providing self-contained and self-sustaining environments for space travel (Gitelson et al., 2003). For quantitative laboratory studies of ecological dynamics, microbial closed ecosystems (CESs) present two main advantages. First, they can sustain diverse microbial populations for years (Brittain, 1993; Folsome and Hanson, 1986) without the need for continued supply of nutrients. Supply of nutrients, such as in conventional chemostat (Becks et al., 2005; Yoshida et al., 2003), periodic refreshment (Price and Morin, 2009; Warren et al., 2003), or serial transfer (Buckling and Rainey, 2002) experiments, necessarily entails the distortion of chemical and spatial interactions, often at a frequency comparable to the measurement frequency. Thus, CESs afford the possibility of unperturbed, long, high-resolution population dynamics measurements under constant

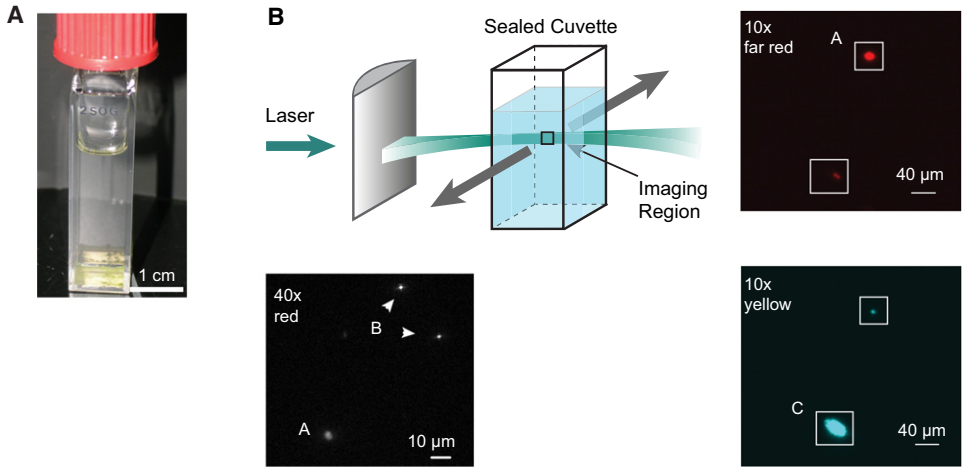

Figure 1. A Synthetic Closed Ecosystem

(A) Example of a closed ecosystem, held in a fluorimetric cuvette.

(B) Density measurements by selective plane illumination microscopy: combined and expanded blue and green laser beams are focused horizontally by a cylindrical lens, producing a thin vertical excitation sheet within the (~5 × 1 × 1 cm) cuvettes in which CESs are enclosed. Fluorescence emission is collected from a central part of the light sheet by long working distance objectives (40×, *E. coli*; 10×, *C. reinhardtii* and *T. thermophila*). Using a dichroic mirror, images of yellow and far-red emission in the same field of view are obtained to improve discrimination of (A) *C. reinhardtii* and (C) *T. thermophila* (top inserts, false colors). *E. coli* (B; arrowheads in lower insert) and *C. reinhardtii* are distinguished by size and brightness in the red emission channel. Direct counting of individuals ensures linearity between culture density and measured cell numbers averaged over a sliding time window.

See also Figure S1 and Table S1.

external conditions. Second, for closed ecosystems, many replicate copies can be readily created with the same initial concentration of nutrients and the same external conditions, permitting accurate separation of population fluctuations from average dynamics and the characterization of these fluctuations in statistical detail (Box 1). Experiments performed for many copies of microbial closed ecosystems have led us to simple quantitative laws describing the nature of random fluctuations in population density.

RESULTS

Our synthetic closed ecosystems consisted of a mixture of three motile microbial species living in a milliliter-size sealed container (Figure 1A) kept at a controlled temperature, and they interacted with the outside environment through absorption of light. The three species were: (1) the green alga *Chlamydomonas reinhardtii*, (2) the Gram-negative bacterium *Escherichia coli*, and (3) the ciliate *Tetrahymena thermophila*. Inspired by previously developed laboratory systems (Kawabata et al., 1995; Nakajima et al., 2009), we chose these three well-studied unicellular species because each of them is motile, can be grown in defined axenic media, is genetically tractable, and does not form spores or cysts. In addition, differences in their sizes, together with the possibility of introducing genes coding for fluorescent proteins into their chromosomes, allowed us to image and automatically count individuals using selective plane illumination microscopy (Huisken et al., 2004) (Figure 1B). Local densities of the three species were measured accurately and noninvasively for months with high temporal resolution in a small, nanoliter-size region inside these containers (see Experimental Procedures; because the measurements are made on an open subsystem of the larger CES, "growth" can be a consequence of division, death, and migration within the CES). Ecosystems were kept under constant illumination and temperature and required no further maintenance. Under these conditions, the three species successfully coexisted in a majority of replicates examined after more than 1,000 days (Figure S1 available online).

A standard view of the ecological interactions taking place in each CES would be to consider the algae as photosynthetic biomass "producers" and the ciliates as "consumers" feeding on bacteria, which, in turn, are "decomposers" of organic debris (Kawabata et al., 1995). Inspection of CES replicates showed, however, that this standard view is rather simplistic. First, in the presence of gravity and thermal convection, each CES quickly became a heterogeneous ensemble of different ecological "niches." For instance, at the bottom of the containers, we observed algae living among debris (Figure 2A), or we observed dense microcolonies of nonswimming bacteria (Figure 2B). Other population heterogeneities were observed on the container walls and at the air-liquid interface. Second, strong phenotypic changes were spontaneously taking place in many CESs. The most notable changes were the appearance of unusually large *T. thermophila*, which were able to ingest algae (Figure 2C; see also Nakajima et al., 2009), and the appearance of filamentous phenotypes of *E. coli* (Figure 2D), which, similarly to the microcolonies, escaped predation by ciliates.

Such phenotypic changes, spontaneous mutations, stochastic divisions, deaths and disintegrations of cells, as well as chemical interactions, through which all three species can affect the growth of others (Matsui et al., 2000; D.R.H. and S.L., unpublished data), are important sources of biological complexity. Replicate CESs differ qualitatively from each other in the range and detailed appearance of these events. For each of the

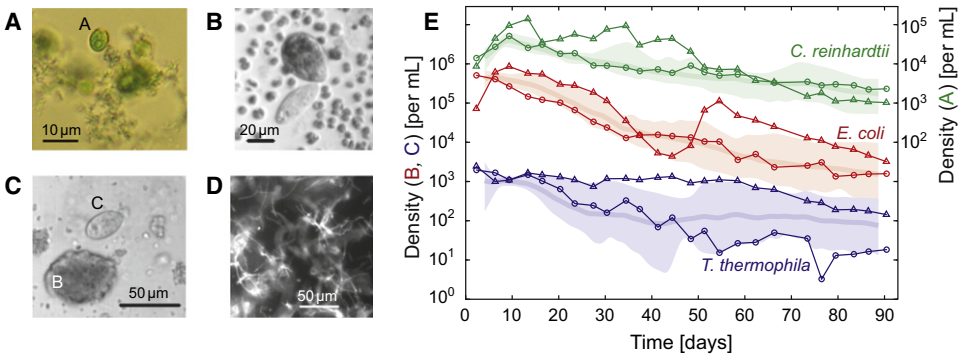

Figure 2. Idiosyncratic Dynamics in a Complex Ecosystem

(A) Live algae (A; *C. reinhardtii*) living among debris, mostly algal cell wall residue.

(B) Large, phase-dense *T. thermophila* (top) eat *C. reinhardtii*, whereas small ones (bottom) do not.

(C) An *E. coli* microcolony (B) next to an individual *T. thermophila* (C).

(D) A mesh of filamentous *E. coli* (red fluorescence channel).

(E) Population dynamics in our replicate CESs under constant light and temperature. Shown are the mean ±bootstrap standard deviation over ecosystems with at least weekly measurements (n = 24), as well as data for two replicates (circles and triangles, respectively). Green (A, right axis): *C. reinhardtii*; red (B): *E. coli*; and blue (C): *T. thermophila*.

systems we could make, at least in principle, a detailed description of the random events or fluctuations that are the substrate for contingency. This historical description would list each microcolony formation, each phenotypic switching event, or each mutation sweeping the population. Then each of these events could be analyzed from a molecular or mechanistic point of view.

Statistical Approach: Replicating Ecosystems

Here, we take a different approach to that of historical description and molecular analysis. By creating many replicates of a simple synthetic CES, we sought to quantitatively characterize the structure of variability in population dynamics. Replicates of ecological systems have rarely been used to this end. In one example, Ramsayer et al. (2012) related variance in stationary-phase density among sets of replicate single- and two-species bacterial ecosystems at different nutrient conditions to the mean density for each condition. The variance of logarithmic density across replicates exhibited power-law scaling with logarithmic mean density, a phenomenon known as Taylor's law (see below; Taylor, 1961). Melbourne and Hastings (2009) studied variability in the rate at which flower beetles invaded replicate laboratory ecosystems, showing that the stochastic components of their model were insufficient to describe all variability. Related questions of historical contingency have received more attention at the level of species composition; much work has shown that the temporal order in which species are added to an ecosystem—its "assembly sequence"—can affect its final species composition, dynamics, and other properties (Sait et al., 2000; Schröder et al., 2005; Jiang et al., 2011).

Variability in population dynamics originates from random fluctuations around the average population dynamics, which are in general time dependent. It is important to distinguish the question of the variability in population dynamics from the usual issue of reproducibility of experiments. We assessed reproducibility by comparing the averaged dynamics of different data sets. Here, local microbial densities in >50 independent replicates of the CES were measured during two independent experiments, lasting ~100 days each, at six measurement frequencies ranging from nearly daily to once every 8 weeks (Figure 3). Densities, averaged over systems measured at least weekly, were found to be almost fully reproducible between the two experiments within the error of the mean (Figure 3). But, while different sets of CES replicates exhibit reproducible *average* dynamics, the local densities of all three species in individual ecosystems fluctuated widely around their slowly varying replicate averages (Figure 2E), resulting in strong variation from one replicate to another.

Do the large fluctuations away from the average dynamics imply that each CES behaves in an idiosyncratic way and that its dynamics do not share common features with other replicates? Possibly not; common ecological interactions could affect the dynamics of all replicate ecosystems, leading to statistical structure in the density fluctuations. In order to uncover such structure, one needs to measure statistical quantities such as covariance, correlation, and scaling exponents. These quantities are of fundamental interest and are not the usual "error bars." Instead, they describe biological variability, which we carefully distinguish from the effects of measurement error and limited sampling (e.g., Figures 3, 4, 5, S2, and S3; Hekstra, 2009).

Variability across Replicate Ecosystems

The availability of detailed time series for replicate systems allows us to characterize the resulting pattern of variability in two ways: by studying variation with time and across replicates (as illustrated in Box 1). To examine the structure of the covariation across replicates first, we examined the behavior of the (3 × 3) correlation matrix of logarithmic densities,

$$C_S^{ij}(t) = \frac{Cov_S(\log n_i, \log n_j)}{\sigma_S(\log n_i) \cdot \sigma_S(\log n_j)},$$

in which $n_i = n_i(t)$ is the density of species i (i = A, B, and C) at time t and log denotes the natural logarithm. The subscript S is

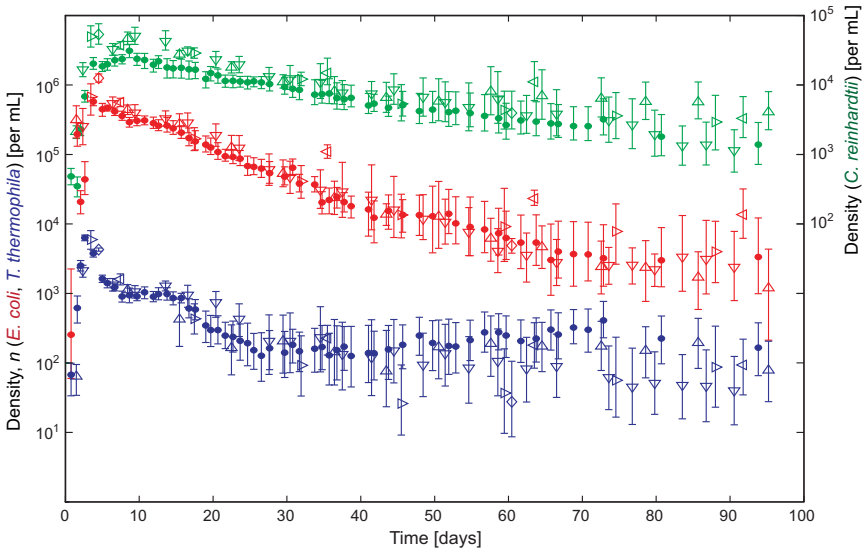

Figure 3. Mean Logarithmic Densities Are Reproducible over Replicate CESs

Shown are mean logarithmic densities per set for experiment 1 (filled circles; one set of nine replicate CESs measured 4–7 times per week) and for experiment 2 (open symbols: five sets of eight to nine systems each, measured at 2 [▽], 1 [△], 1/2 [▷], 1/4 [◁], and 1/8 [◇] week^{-1}), with 90% bootstrap confidence intervals for the mean (Experimental Procedures).

At the p = 0.05 significance level (not adjusted for multiple testing, by two-sided test), for 3 out of 36 comparisons (12 time points × 3 species), the mean logarithmic densities differ significantly between the two experiments (n = 9, 15 systems tested by bootstrapping; time points before 10 days were excluded).

a reminder that we are considering the statistics over replicate systems. The composition of the three eigenvectors of $C_S(t)$ stabilizes over time (Figure 4A) and is reproducible between the two experiments (compare circles, triangles, and squares in Figure 4A). In addition, the corresponding eigenvalues of $C_S(t)$ are stable and well separated after ~3 weeks (Figure 4B). In other words, we can represent observations of $\log(n_A, n_B, n_C)$ as clouds of points, which have their "orientation axes" and their relative sizes along these orientations, stable in time (cf. Box 1, panel F). Given this separation and relative stability, we propose to refer to these eigenvectors, or axes, as ecomodes and classify them according to their eigenvalues (Figure 4): small (S), medium (M), and large (L). We can now examine fluctuations along each of these ecomodes. The L ecomode represents collective fluctuations of the three species, likely a common occurrence in ecosystems (Houlahan et al., 2007). The M ecomode shows fluctuations of *E. coli* opposite to fluctuations of the other two species. The S ecomode, necessarily, describes the remaining fluctuations, mostly between *C. reinhardtii* and *T. thermophila*.

The L ecomode describes ~60% of correlation in logarithmic population densities (Figure 4B). Because of this dominance of the L ecomode, species densities in the same ecosystem tend, at any given moment, to be on the same side of their respective replicate averages (for example, see Figure 2E). If the L ecomode had represented all correlation and variance, one would have seen the densities of the three species in individual CESs fluctuate in lock-step relative to their respective replicate averages. However, consistent with the nonzero contribution of the M ecomode (20%–30% of correlation), independent fluctuations, especially of *E. coli*, do occur (e.g., in Figure 2E over days 30–60). Interestingly, in a series of independent, exploratory experiments, we observed that both *T. thermophila* and *C. reinhardtii* strongly suppressed *E. coli* average densities in two-species systems relative to single-species systems (D.R.H. and S.L., unpublished data).

Underlying these ecomodes is an accumulation of variance across systems, resulting from instantaneous growth rate fluctuations of individual species in individual ecosystems. To understand this accumulation, we asked how fast density fluctuations along each ecomode tend to revert to the replicate average ("revert to the mean"), $\langle \log n \rangle$, by calculating autoregressive coefficients b along each ecomode (Supplemental Information and Box 1). We found that fluctuations along the S and M ecomodes revert to the mean on a timescale $\tau \approx \Delta t/(1-b) \approx 3$ and 6 weeks, respectively. For the largest ecomode, $b \approx 1$ and τ is very large, allowing variance along the L ecomode to accumulate throughout each 3 month long experiment. The inclusion of delayed-interaction terms in the data description does not change our conclusions (see Extended Experimental Procedures).

The ecomode structure in the covariance across replicates shows a striking and nontrivial relationship with the covariation of species densities with time. Covariation across time is conventionally analyzed by estimating the species interaction matrix, B (Ives et al., 2003), which describes the short-term (here, weekly) structure of simultaneous growth rate fluctuations of the different species (illustrated in Box 1). Remarkably, for our data, the ecomodes resemble the eigenvectors of the interaction matrix quite accurately, and the ecomode autoregressive coefficients b, considered above, accurately match the eigenvalues of the interaction matrix, B (Figure 4C). In other words, one could, surprisingly, learn about the interactions between the species within ecosystems by studying the differences in observed species densities among replicates at a single point in time or vice versa. This is by no means a necessary outcome. For example, long-term correlations or periodicity in growth rate fluctuations could have dominated the long-term covariance across replicates and led to a different outcome (for more detail, see the Extended Experimental Procedures). The possibility of a close correspondence between ecomodes and the eigenvectors of the interaction matrix is implied by previous theoretical work (Ives, 1995; Ives et al., 2003). However, to our knowledge, this is the first experimental demonstration of this correspondence.

Properties of Temporal Fluctuations

The fact that, on the timescale of the experiments, the fluctuations along the L ecomode do not revert back to the mean is

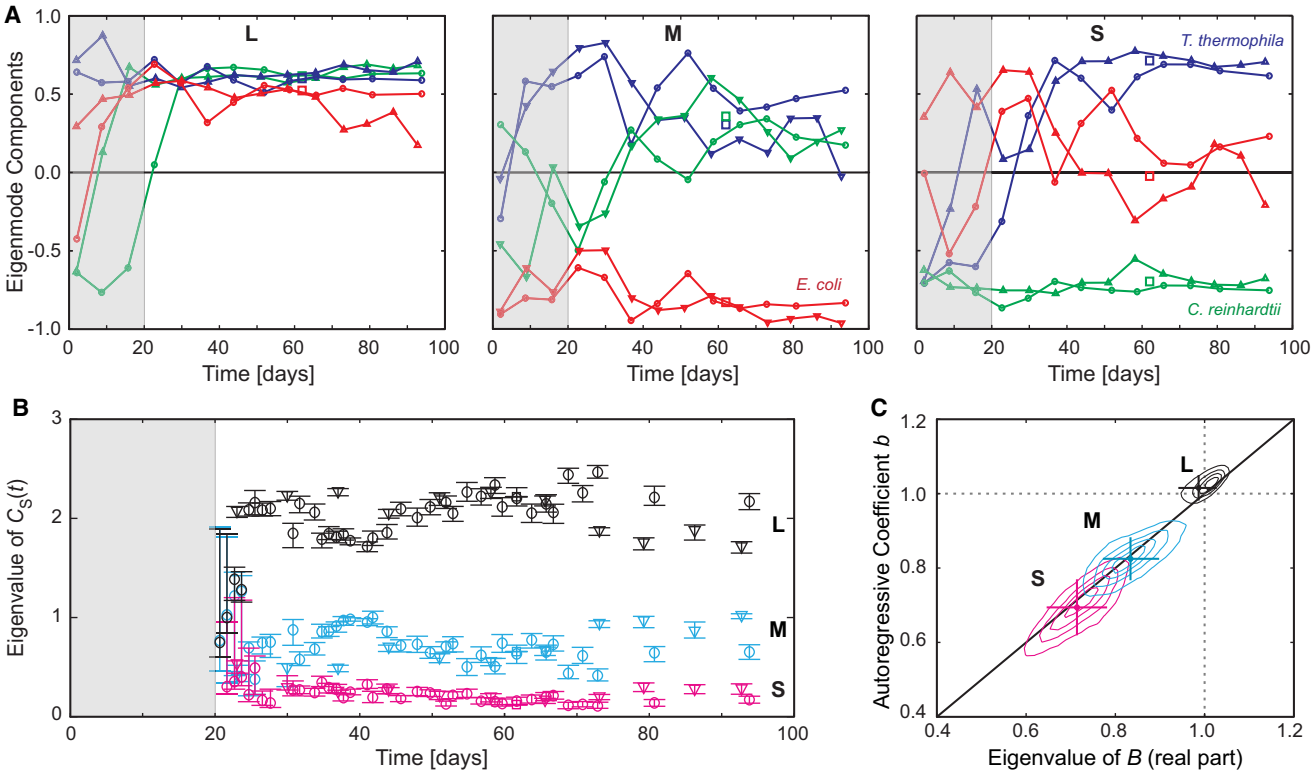

Figure 4. Ecomodes

(A) Composition of ecomodes, the eigenvectors of the correlation matrix C_S, was determined at weekly time points and associated between subsequent time points based on similarity (inner products). Shown for experiments 1 (circles: n = 9) and 2 (triangles: measured once or twice per week, n = 15; squares at day 62: for CESs measured once per 4 or 8 weeks, n = 17). Ecomodes are labeled L, M, and S according to their corresponding eigenvalues in (B). Within the shaded areas, eigenvalues are not clearly separated and ecomodes are hence poorly defined. Green, *C. reinhardtii*; red, *E. coli*; blue, *T. thermophila*; species names added for clarity.

(B) Dynamics of the eigenvalues of C_S in experiments 1 and 2 (symbols as in A). Eigenvalues are labeled L (large, black), M (medium, cyan), and S (small, magenta). Error bars indicate bootstrap standard errors.

(C) Autoregressive coefficients b measured along ecomodes closely match the eigenvalues of the interaction matrix B. Estimation of B (here with Δt = 1 week) is illustrated in Box 1 and explained in the Supplemental Information. Shown are isoprobability contours as well as means and SEs, all obtained by bootstrapping. See also Figure S2 and Table S2.

a telltale sign of nonstationarity. Such nonstationarity can limit the long-term predictability of ecological dynamics. Characterizing this nonstationarity, we found that growth rate fluctuations of each species display little memory and have fairly stable variance (Figure S3). These observations imply that the population dynamics of all three species in individual ecosystems should approach a "geometric random walk" (log n presents random walk behavior) around the replicate-average dynamics (Herrndorf, 1984; Niwa, 2007).

For such random walks, one also expects that the size of logarithmic density fluctuations, $\sigma(\Delta \log n - \Delta\langle \log n\rangle)$, as a function of time interval Δt, should grow as a power law Δt^H, with the so-called Hurst exponent (Feder, 1988) H = 1/2 in the absence of measurement error. Thus, a plot of the logarithm of the size of fluctuations, $\log(\sigma(\Delta \log n - \Delta\langle \log n\rangle))$, against the logarithm of Δt should yield a straight line with slope H. From Figure 5A we can see that, indeed, each species quite closely follows power-law behavior expected for random walks (estimated exponents are somewhat smaller than 1/2 in the presence of measurement error; see Extended Experimental Procedures). In addition, we confirmed this geometric random walk behavior by performing high temporal resolution density measurements on a single replicate CES over an extra 8 weeks (data not shown). The power spectrum, S, of the acquired logarithmic density time series exhibited a power-law decay with temporal frequency f, i.e., $S(f) \propto f^{-\alpha}$, with the exponent α close to 2, as expected for random walks (Figure 5B).

Remarkably, temporal dynamics of population densities displayed an additional type of scaling. Density fluctuations, Δn, themselves scale with mean density with an exponent, β, close to 1, providing a dynamical example of Taylor's law (Figure 5C; Eisler et al., 2008; Taylor, 1961). This implies that the size of fluctuations in log n depends only very weakly on density (to see this, note that $\Delta \log(n) \approx \Delta n/n$, so fluctuations in log n scale as $n^{\beta-1} \approx n^0$). This observation suggests that it is the growth rate fluctuations of the whole measured population that dominate variability, rather than the combination of many individual-level fluctuations (which would lead to an exponent, β = 1/2, as

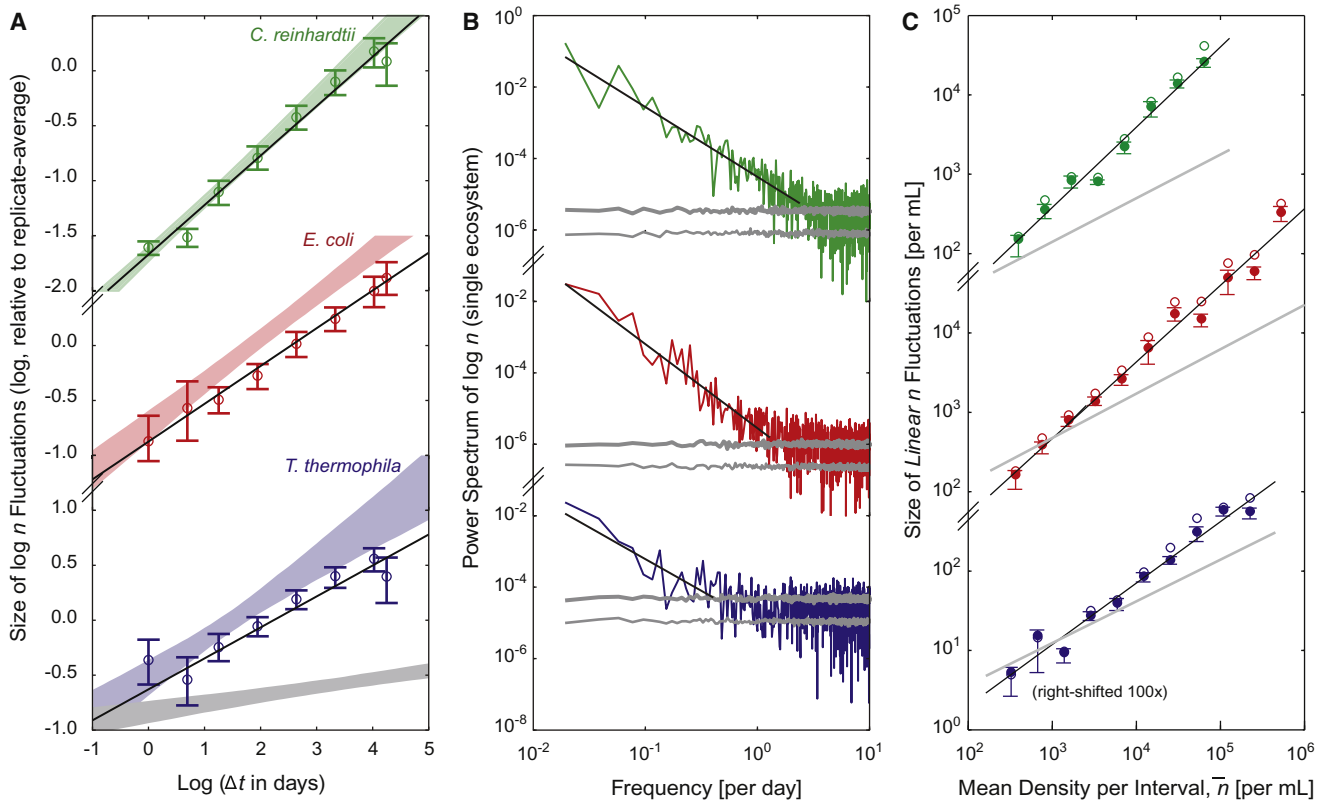

Figure 5. Scaling of Density Fluctuations with Time and Density

(A) The size of density fluctuations scales with time lag Δt as $\sigma(\Delta \log n - \Delta\langle \log n\rangle) \propto \Delta t^H$, with Hurst exponent H. Scaling is compared to synthetic random walks with the same observed growth rate fluctuations, measurement schedule, and measurement error (colored areas, ±1 SE of the least-squares fit). Scaling in the absence of growth rate fluctuations is indicated in gray for *T. thermophila* (not shown for *C. reinhardtii* and *E. coli*, for which it is smaller). Estimates of H are 0.45 ± 0.03 for *C. reinhardtii*, 0.34 ± 0.06 for *E. coli*, and 0.28 ± 0.06 for *T. thermophila*. Deviations from 0.50 are due in large part to their sensitivity to measurement error (Supplemental Information).

(B) Power spectra for log n in a single closed ecosystem during days 122–175, based on continuous density measurements. Where power exceeds counting noise, it scales with frequency (black regression lines, 1/4 $S(f) \propto f^{-\alpha}$). Gray lines: 95% level and median measurement error. Estimates of α are 1.95 ± 0.08 for *C. reinhardtii*, 2.27 ± 0.13 for *E. coli*, and 1.78 ± 0.30 for *T. thermophila*.

(C) Density fluctuations scale with density. Mean (linear) density, $\overline{n} = 1/2(n(t+\Delta t) + n(t))$, and change in density, $\Delta n = n(t+\Delta t) - n(t)$, were determined for pairs of density measurements Δt = 1 week apart (n = 279, first week excluded) and binned by $\overline{n}$. Shown is $\sigma(\Delta n)$, with SE, versus $\overline{n}$, before (open circles) and after (filled circles) correction of Δn for the change in replicate average, $\Delta\langle n\rangle$. Gray lines: expected contribution of measurement error.

Green, *C. reinhardtii*; red, *E. coli*; and blue, *T. thermophila*. Estimates of the scaling exponent, β, are 1.03 ± 0.06 for *C. reinhardtii*, 0.99 ± 0.06 for *E. coli*, and 0.79 ± 0.05 for *T. thermophila*. See also Figure S3.

seen in the addition of independent random variables). We emphasize the difference with the common "static" version of Taylor's law, which describes the scaling of the variance of density or abundance, rather than that of density fluctuations, with mean density (Eisler et al., 2008).

Without the possibility of creating and controlling ecosystem replicates, it is difficult to quantitatively address fundamental questions, for example, the question about the relative role of endogenous and exogenous factors (Ives et al., 2003; Melbourne and Hastings, 2009) (often, for instance, the weather). In our CESs, differences in seal quality between replicate ecosystems unexpectedly already provided a hint of such an approach. Residual gas exchange through the seal resulted in a tiny but measurable loss of water (<0.1 mg/day; Figure S2A), explaining some variation in species densities across CESs (Figure S2B). Resulting variation among replicates aligns mainly with the large ecomode (L; Figure S2C). Although more systematic studies are needed, this observation suggests that variation along the large ecomode reflects variation in the availability of a resource affected by residual gas exchange (e.g., carbon dioxide). Removal of this exogenous factor in the statistical analysis did not significantly change the nature and dynamics of the observed three ecomodes (Figures S2D and S2E).

DISCUSSION

It is difficult to imagine how ecological observations and measurements performed outside of the laboratory could allow us to systematically address the problem of contingency, i.e., long-lasting dependence on past random events. Even for measurements performed in conditions carefully selected for their similarity (e.g., on islands with similar biogeographical and

climatic conditions), one can never be sure that the observed variability did not originate in interactions with an unknown component or in some extrinsic perturbations that were present for some of the measurements and not for the others. (We note that this makes observed cases of ecological convergence [Losos and Ricklefs, 2009] all the more striking.)

On the other hand, creation of easily replicated microbial closed ecosystems with well-controlled initial and external conditions allowed long-term measurements of the dynamics of interacting populations with reproducible average dynamics. This led us to establish two simple statistical results describing the nature of random fluctuations around the average dynamics. First, despite wide variations of the population dynamics in individual systems around their mean and an increase of variance with time, the variations of the three species were correlated. Well-defined ecomodes that describe these correlations emerged and stabilized after an initial period of about 3 weeks. The existence of these ecomodes reflects the fact that fluctuations of the three species' densities around the replicate-average dynamics are coupled through ecological interactions that are common to all replicates. Second, despite the large complexity of biological phenomena observed in individual ecosystems, it was, remarkably, possible to describe the resulting fluctuations in population dynamics by simple quantitative laws. Specifically, local population dynamics displayed power-law behavior close to a geometric random walk around the average dynamics. Underlying these random walks is a single dominant ecomode, along which density fluctuations do not revert to the mean.

It would be intriguing to see whether these results are of a general nature. For instance, geometric random walks and dominant collective modes have been observed in historical time series generated by multiplicative, noisy processes, such as finance (Laloux et al., 1998; Mantegna and Stanley, 1999), which suggests the possibility of common underlying mechanisms and the development of ecological theory. In particular, a system undergoing a random walk is clearly contingent; the effects of some random events do not die away exponentially fast, as in stationary processes, but instead they persist. At the same time, these effects are not amplified exponentially, as is the case for chaotic systems (Kantz and Schreiber, 2004). Ecological and evolutionary dynamics can take place on similar timescales (Yoshida et al., 2003). It is tempting to speculate that contingency is a consequence of underlying genetic and phenotypic change in a multispecies ecosystem and, in turn, affects these processes, as populations modify each other's environment.

On the other hand, recently observed extreme repeatability of temporal dynamics and spatial patterns in similar experiments involving long-term single-species dynamics (Frentz et al., 2010) shows that the number of interacting components, the nature of their interactions, or the details of starting or external conditions may play a crucial role (cf. Jiang et al., 2011). It is very likely that emergent ecological laws will not be as simple as the Gutenberg-Richter law that describes the distribution of earthquakes. However, it is our view that, by introducing and quantitatively analyzing the effects of physical and genetic perturbations and by modifying the composition of the CESs, one should be able to probe the underlying sources and consequences of contingency and determine to what extent the uncovered quantitative laws for ecological fluctuations are universal.

EXPERIMENTAL PROCEDURES

Strain Construction

E. coli MG1655 Δ*flu* Δ*fimA* att_{HK022}::(*cat* $P_{\lambda R}$-*dTomato*) *hsdR514* was constructed in two steps. (1) *flu*, the gene for the Ag43 cell-cell adhesion protein (Hasman et al., 2000) and *fimA*, encoding the structural unit of fimbriae (Hasman et al., 2000), fimA, were deleted by P1 transduction from Keio-collection deletion strains (Baba et al., 2006) to an MG1655 recipient. After the first transduction, the kanamycin marker was removed (Baba et al., 2006). *hsdR514* was cotransduced from the donor strain and retained as a marker. (2) pZS* (att_{HK022}) 3R dTomato was constructed by insertion of the dTomato open reading frame (ORF) (Shaner et al., 2004) between KpnI and HindIII restriction sites of a pZS* plasmid (Lutz and Bujard, 1997) containing a phage HK022 attachment site. After excision of the origin of replication, a (*cat* $P_{\lambda R}$-*dTomato*) fragment was integrated at the chromosomal att site (Haldimann and Wanner, 2001) in MG1655. The (*cat* $P_{\lambda R}$-*dTomato*) fragment was then P1 transduced to the strain resulting from step (1). No loss of fluorescent marker was observed after 200 days.

Chlamydomonas reinhardtii strain UTEX 2244 (mt+, UT Austin Culture Collection) is naturally fluorescent (chlorophyll). Construction of *T. thermophila* H3.2-EYFP followed (Liu et al., 2004), except that the somatic rescue plasmid contained the wild-type *HTT2/HHF2* locus with a 6 amino acid linker (DPPVAT) and the EYFP-coding sequence, derived from pYFP-URA3 (Gerami-Nejad et al., 2001) and inserted into *HHT2* before its stop codon. The fluorescence marker was stable during 16 months of monthly subculture.

Ecosystem Construction

Single-species cultures were grown to late exponential phase for *C. reinhardtii* in Tris-acetate-phosphate (TAP) (Volvocales Information Project, http://www.unbf.ca/vip/), *T. thermophila* in supplemented proteose peptone (SPP) (Asai and Forney, 2000), and *E. coli* in 1/2× Taub #36 with 0.03% proteose peptone number 3 (Taub medium; Taub and Dollar, 1964). Cultures were tested for purity by visual inspection and plating on four solid media and were washed twice in Taub medium. Glassware for preparation of Taub medium and fluorimetric cuvettes (Special Optical Glass, Starna Cells), in which systems were kept, was cleaned in ≥10% HNO_3 at least overnight, rinsed in ddH_2O, rinsed three times with isopropanol (or kept over boiling 200 proof ethanol), rinsed with ddH_2O, and autoclaved. From a master mix of Taub medium with 5,000 ml^{-1} *C. reinhardtii*, 500 ml^{-1} *E. coli*, and 50 ml^{-1} *T. thermophila*, 3 ml was pipetted into each cuvette, and cuvettes were sealed by tightening the screw caps. In the first experiment, 11 systems were constructed, and in 9 of those systems, densities were measured. In the second experiment, 5 sets of 10 ecosystems were constructed (systems losing >0.1 mg/day water were excluded from analysis; loss rates were stable over time; Figure S2A).

Ecosystems were kept in sample stands at 1,200 lux ± 10% (white BW03 light-emitting diodes [LEDs], Lumileds; temporal variability <1%, homogenized using two diffusive screens), and 23.1°C ± 0.1°C (max. ΔT <80 mK within and between sample locations). Long-term coexistence was assessed visually on an inverted microscope and (experiment 1) by subculturing and plating on solid media.

Selective Plane Illumination Microscopy

The principle of selective plane illumination microscopy (SPIM) is illustrated in Figure 1B. Beams from 473 nm (Lasever, 20 mW) and 532 nm (AOTK, 50 mW) diode-pumped solid state (DPSS) lasers were combined into a single beam using a 495 nm long-pass dichroic that was expanded by a 10× beam expander (Newport), constricted using an 8 mm diameter iris, and focused by a cylindrical lens (f = 80 mm, Thorlabs) with antireflective coating. Electronic shuttering was performed using a Pockels cell with integral polarizer (ConOptics), yielding an extinction ratio of ~200×. Fluorescence emission was collected centrally, 5 mm below the meniscus, by using, for *C. reinhardtii*

and *T. thermophila*, a 10× infinity-corrected CF Plan Mitutoyo objective (nominal NA = 0.30, working distance = 16.5 mm) and, for *E. coli*, an M Plan 40× ELWD Nikon objective (nominal NA = 0.5, working distance = 11 mm). Objective position was controlled using Mitutoyo linear stages. Light from the 10× objective was split by a 45° 660 nm long-pass dichroic. Objectives were used at reduced tube length (from base of the objective to camera), yielding effective magnifications of 15× and 6×, respectively. Red fluorescence emission was collected on an uncooled Retiga EXi camera (QImaging) with D620/60 emission filter. Yellow and far-red emissions were collected on CV-M10SX cameras (JAI) with HQ515/30 and custom 665LP filters, respectively (all filters and dichroics: Chroma Technology).

On measurement days, each cuvette was placed in the SPIM, flow was allowed to subside for $\geq$3 min, and images were taken at $\sim$1.2 Hz with an exposure time of 35 ms (between acquisitions, the sample was illuminated with white light as in the sample stands). The temperature in the SPIM was 25.5°C. A typical measurement consisted of 2,000–5,000 images (30–60 min).

Image and Statistical Analysis

Objects in images were identified in ImagePro Plus 4.5 (Media Cybernetics), and object properties were written to file. Additional thresholds were applied in Matlab 6.1 (Mathworks). Thresholds were validated by inspection of performance on images acquired from pure and mixed cultures. All density estimates are based on averages over thousands of images. When considering log n, 0 counts were replaced by half counts. The null model for measurement error (dominated by serial correlation between counts [Hekstra, 2009]) assumes that individuals enter the field of view independently at a rate that is proportional to their local density and that they leave it at a constant rate. The model (Hekstra, 2009) approaches a Poisson distribution for total counts over time windows larger than a few seconds for an effective number of samples set by the average residence time of individuals in the observation volume.

Confidence intervals for most quantities were determined by bootstrapping (Efron and Gong, 1983) to minimize imposition of statistical structure on the data. Bootstrapping was performed by resampling with replacement the set of observed densities at each time point at least 500 (for SE) or 1,000 times (for 90% confidence intervals). Each bootstrap sample consisted of the same number of measurements as the data, with measurement error added by sampling the null model mentioned above. "Bootstrap standard errors" are 15.9%–84.1% confidence intervals and can be asymmetric. To determine confidence intervals for quantities evaluated over entire time series, the bootstrapping procedure samples entire time series at once. Exponents were estimated by ordinary least-squares regression on log-transformed variables and were corrected for bias where necessary (Sprugel, 1983). All operations were performed in Matlab by using custom scripts.

SUPPLEMENTAL INFORMATION

Supplemental Information includes Extended Experimental Procedures, three figures, and two tables and can be found with this article online at doi:10.1016/j.cell.2012.03.040.

ACKNOWLEDGMENTS

We thank for comments and suggestions: S. Cocco, J. Cohen, S. Dutcher, J. Hopfield, D. Huse, G. Iyengar, A. Libchaber, J. McKinney, R. Monasson, R. Ranganathan, T.N. Siegel, and M.-C. Yao, as well as current and former members of our laboratory; for technical assistance: J. Chuang, Y. Liu, and S. Ram; and for distribution of genetic constructs and strains: the laboratories of C.D. Allis, J. Berman, and R. Tsien and the Yale Coli Genetic Stock Center, the National BioResource Project (NIG, Japan), and the Culture Collection of Algae (UT Austin). D.R.H. acknowledges support from the Training Program in Chemical Biology.

Received: December 19, 2011
Revised: February 10, 2012
Accepted: March 9, 2012
Published: May 24, 2012

REFERENCES

Asai D.J. and Forney J.D., eds. (2000). Tetrahymena thermophila in Methods in Cell Biology (San Diego: Academic Press).

Baba, T., Ara, T., Hasegawa, M., Takai, Y., Okumura, Y., Baba, M., Datsenko, K.A., Tomita, M., Wanner, B.L., and Mori, H. (2006). Construction of *Escherichia coli* K-12 in-frame, single-gene knockout mutants: the Keio collection. Mol. Syst. Biol. *2*, 2006.0008.

Bak, P., and Paczuski, M. (1995). Complexity, contingency, and criticality. Proc. Natl. Acad. Sci. USA *92*, 6689–6696.

Becks, L., Hilker, F.M., Malchow, H., Jürgens, K., and Arndt, H. (2005). Experimental demonstration of chaos in a microbial food web. Nature *435*, 1226–1229.

Blount, Z.D., Borland, C.Z., and Lenski, R.E. (2008). Historical contingency and the evolution of a key innovation in an experimental population of *Escherichia coli*. Proc. Natl. Acad. Sci. USA *105*, 7899–7906.

Bretz, M., Zaretzki, R., Field, S.B., Mitarai, N., and Nori, F. (2006). Broad distribution of stick-slip events in slowly sheared granular media: table-top production of a Gutenberg-Richter-like distribution. Europhys. Lett. *74*, 1116–1122.

Brittain, A.M. (1993). The metabolic diversity, biological activity, and stability of the steady state condition in closed ecosystems. PhD thesis, University of Hawaii, Honolulu, HI.

Buckling, A., and Rainey, P.B. (2002). The role of parasites in sympatric and allopatric host diversification. Nature *420*, 496–499.

Carlson, J.M., and Langer, J.S. (1989). Mechanical model of an earthquake fault. Phys. Rev. A *40*, 6470–6484.

Efron, B., and Gong, G. (1983). A leisurely look at the bootstrap, the jackknife, and cross-validation. Am. Stat. *37*, 36–48.

Eisler, Z., Bartos, I., and Kertesz, J. (2008). Fluctuation scaling in complex systems: Taylor's law and beyond. Adv. Phys. *57*, 89–142.

Feder, J. (1988). Fractals (New York: Plenum Press).

Folsome, C.E., and Hanson, J.A. (1986). The emergence of materially-closed-system ecology. In Ecosystem Theory and Applications, N. Polunin, ed. (New York: John Wiley & Sons).

Frentz, Z., Kuehn, S., Hekstra, D., and Leibler, S. (2010). Microbial population dynamics by digital in-line holographic microscopy. Rev. Sci. Instrum. *81*, 084301.

Gerami-Nejad, M., Berman, J., and Gale, C.A. (2001). Cassettes for PCR-mediated construction of green, yellow, and cyan fluorescent protein fusions in *Candida albicans*. Yeast *18*, 859–864.

Gitelson, I.I., Lisovsky, G.M., and MacElroy, R.D. (2003). Manmade Closed Ecological Systems (London and New York: Taylor & Francis).

Gould, S.J. (1989). Wonderful Life: The Burgess Shale and the Nature of History (New York: W.W. Norton & Co.).

Haldimann, A., and Wanner, B.L. (2001). Conditional-replication, integration, excision, and retrieval plasmid-host systems for gene structure-function studies of bacteria. J. Bacteriol. *183*, 6384–6393.

Hasman, H., Schembri, M.A., and Klemm, P. (2000). Antigen 43 and type 1 fimbriae determine colony morphology of *Escherichia coli* K-12. J. Bacteriol. *182*, 1089–1095.

Hekstra, D.R. (2009). Population dynamics in a model closed ecosystem, PhD Thesis, The Rockefeller University, New York, NY.

Herrndorf, N. (1984). A functional central limit theorem for weakly dependent sequences of random variables. Ann. Probab. *12*, 141–153.

Houlahan, J.E., Currie, D.J., Cottenie, K., Cumming, G.S., Ernest, S.K.M., Findlay, C.S., Fuhlendorf, S.D., Gaedke, U., Legendre, P., Magnuson, J.J., et al. (2007). Compensatory dynamics are rare in natural ecological communities. Proc. Natl. Acad. Sci. USA *104*, 3273–3277.

Huisken, J., Swoger, J., Del Bene, F., Wittbrodt, J., and Stelzer, E.H.K. (2004). Optical sectioning deep inside live embryos by selective plane illumination microscopy. Science *305*, 1007–1009.

Ives, A.R. (1995). Measuring resilience in stochastic systems. Ecol. Monogr. *65*, 217–233.

Ives, A.R., Dennis, B., Cottingham, K.L., and Carpenter, S.R. (2003). Estimating community stability and ecological interactions from time-series data. Ecol. Monogr. *73*, 301–330.

Jiang, L., Joshi, H., Flakes, S.K., and Jung, Y. (2011). Alternative community compositional and dynamical states: the dual consequences of assembly history. J. Anim. Ecol. *80*, 577–585.

Kantz, H., and Schreiber, T. (2004). Nonlinear Time Series Analysis, Second Edition (Cambridge: Cambridge University Press).

Kawabata, Z., Matsui, K., Okazaki, K., Nasu, M., Nakano, N., and Sugai, T. (1995). Synthesis of a species-defined microcosm with protozoa. J. Protozool. Res. *5*, 23–26.

Laloux, L., Cizeau, P., Bouchaud, J.P., and Potters, M. (1998). Noise dressing of financial correlation matrices. Phys. Rev. Lett. *83*, 1467–1470.

Liu, Y.F., Mochizuki, K., and Gorovsky, M.A. (2004). Histone H3 lysine 9 methylation is required for DNA elimination in developing macronuclei in *Tetrahymena*. Proc. Natl. Acad. Sci. USA *101*, 1679–1684.

Losos, J.B., and Ricklefs, R.E. (2009). Adaptation and diversification on islands. Nature *457*, 830–836.

Lutz, R., and Bujard, H. (1997). Independent and tight regulation of transcriptional units in Escherichia coli via the LacR/O, the TetR/O and AraC/I_1-I_2 regulatory elements. Nucleic Acids Res. *25*, 1203–1210.

Mantegna, R.N., and Stanley, H.E. (1999). An Introduction to Econophysics: Correlations and Complexity in Finance (Cambridge, UK: Cambridge University Press).

Matsui, K., Kono, S., Saeki, A., Ishii, N., Min, M.G., and Kawabata, Z. (2000). Direct and indirect interactions for coexistence in a species-defined microcosm. Hydrobiologia *435*, 109–116.

Melbourne, B.A., and Hastings, A. (2009). Highly variable spread rates in replicated biological invasions: fundamental limits to predictability. Science *325*, 1536–1539.

Morris, S.C. (2010). Evolution: like any other science it is predictable. Philos. Trans. R. Soc. Lond. B Biol. Sci. *365*, 133–145.

Mrozek, S. (1968). The Ugupu bird. In The Ugupu Bird, translated from the Polish by K. Syrop (London: MacDonald), pp. 39–43.

Nakajima, T., Sano, A., and Matsuoka, H. (2009). Auto-/heterotrophic endosymbiosis evolves in a mature stage of ecosystem development in a microcosm composed of an alga, a bacterium and a ciliate. Biosystems *96*, 127–135.

Niwa, H.S. (2007). Random-walk dynamics of exploited fish populations. ICES J. Mar. Sci. *64*, 496–502.

Price, J.E., and Morin, P.J. (2009). Community convergence in a simple microbial food web. Ecol. Res. *24*, 587–595.

Ramsayer, J., Fellous, S., Cohen, J.E., and Hochberg, M.E. (2012). Taylor's Law holds in experimental bacterial populations but competition does not influence the slope. Biol. Lett. *8*, 316–319.

Sait, S.M., Liu, W.-C., Thompson, D.J., Godfray, H.C.J., and Begon, M. (2000). Invasion sequence affects predator-prey dynamics in a multi-species interaction. Nature *405*, 448–450.

Schröder, A., Persson, L., and De Roos, A.M. (2005). Direct experimental evidence for alternative stable states: a review. Oikos *110*, 3–19.

Sethna, J.P., Dahmen, K.A., and Myers, C.R. (2001). Crackling noise. Nature *410*, 242–250.

Shaner, N.C., Campbell, R.E., Steinbach, P.A., Giepmans, B.N.G., Palmer, A.E., and Tsien, R.Y. (2004). Improved monomeric red, orange and yellow fluorescent proteins derived from *Discosoma* sp. red fluorescent protein. Nat. Biotechnol. *22*, 1567–1572.

Sprugel, D.G. (1983). Correcting for bias in log-transformed allometric equations. Ecology *64*, 209–210.

Taub, F.B., and Dollar, A.M. (1964). A *Chlorella-Daphnia* food-chain study: the design of a compatible chemically defined culture medium. Limnol. Oceanogr. *9*, 61–74.

Taylor, L.R. (1961). Aggregation, variance and mean. Nature *189*, 732–735.

Warren, P.H., Law, R., and Weatherby, A.J. (2003). Mapping the assembly of protist communities in microcosms. Ecology *84*, 1001–1011.

Yoshida, T., Jones, L.E., Ellner, S.P., Fussmann, G.F., and Hairston, N.G., Jr. (2003). Rapid evolution drives ecological dynamics in a predator-prey system. Nature *424*, 303–306.